ADVANCED MATERIALS
www.advmat.de

Twisted Acoustics: Metasurface-Enabled Multiplexing and Demultiplexing

Xue Jiang, Bin Liang, Jian-Chun Cheng,* and Cheng-Wei Qiu**

Metasurfaces are used to enable acoustic orbital angular momentum (a-OAM)-based multiplexing in real-time, postprocess-free, and sensor-scanning-free fashions to improve the bandwidth of acoustic communication, with intrinsic compatibility and expandability to cooperate with other multiplexing schemes. The metasurface-based communication relying on encoding information onto twisted beams is numerically and experimentally demonstrated by realizing real-time picture transfer, which differs from existing static data transfer by encoding data onto OAM states. With the advantages of real-time transmission, passive and instantaneous data decoding, vanishingly low loss, compact size, and high transmitting accuracy, the study of a-OAM-based information transfer with metasurfaces offers new route to boost the capacity of acoustic communication and great potential to profoundly advance relevant fields.

Acoustic communication is pivotal in applications such as ocean exploration, where sound is the dominant information carrier due to the prominent loss of light in ocean.[1–3] Unlike optical communication with the high frequency and light speed, data transfer based on sound is subject to deficiencies of low frequency and velocity, limiting the advancement of acoustic communication.[1–3] Although remarkable progress has been made by introducing wavelength-division multiplexing (WDM), time-division multiplexing (TDM), and multilevel amplitude/phase modulation,[4–7] data rate of acoustic communication is approaching its current limit, due to the fact that sound, as a scalar wave, bears no polarization or spin, as opposed to its optical counterparts. It is stringent to exploit plausible multiplexing mechanisms to encode information in a scalar field with multiple states orthogonal and compatible to existing degrees of freedom (DOF). Orbital angular momentum (OAM), with the infinite dimensionality of its Hilbert space, is a promising candidate.

Many efforts have been made in optical OAM-based multiplexing,[8] such as spiral phase masks,[9,10] Dammann gratings,[11,12] q-plates,[13] or interferometers.[14] The precise control of sound would result in bulky device if we directly translate the optical mechanisms into acoustics. Previous works on acoustic OAM (a-OAM) beams[15,16] primarily exploit the mechanical effects,[17–20] only one work has attempted to utilize OAM in acoustic communication.[21] However, the method in ref. [21] relies on encoding data on OAM states and only employs this single dimension to have a static data transfer, while the fast and continuous communication should work in a real-time manner. In addition, an active sensors array and complex algorithms are required for field scanning and data decoding, which not only impose extra loads both in hardware and software, but also limit the transmission speed due to the time consumption in postdata processing. The active decoding also restricts the transmission accuracy since the bit error rate is highly dependent on the transducers number in the sensor array.[21]

We theoretically propose and experimentally validate the twisted beam carrying OAM for real-time acoustic communication in a passive, postprocess-free, and sensor scanning-free paradigm with metasurfaces[22–27] to overcome those aforementioned issues. Rather than encoding data onto OAM states (i.e., "on–off" of OAM states represent "1–0"), we utilize the twisted beams as the data carriers where OAM, phase, amplitude, and frequency are the basic properties of beams and encode data parallel onto these dimensions, exhibiting the instinct compatibility with preexisting DOF. We enter the null of the twisted beams associated with the spiral phase $e^{im\theta}$ (m is topological charge and θ is azimuthal angle) and take full advantage of this characteristic, which is usually less significant. An acoustic demultiplexing metasurface (a-DMM) with a 0.5λ thickness and 0.53λ radius (λ is sound wavelength), as a passive and compact component, is proposed to directly and promptly decode data by a single transducer. Comparisons among our a-DMM-based communication with metasurfaces, the methods in ref. [21] and other milestone references are shown in **Figure 1**a. The pressure transmittance is 91.5% for one a-DMM and a nearly 100% transmission accuracy is achieved. Advantages of free of postprocess and field scanning, passiveness and compactness, high capacity and accuracy in real-time manner will be demonstrated in what follows.

Dr. X. Jiang, Prof. B. Liang, Prof. J.-C. Cheng
Collaborative Innovation Center of Advanced Microstructures and Key Laboratory of Modern Acoustics
MOE
Institute of Acoustics
Department of Physics
Nanjing University
Nanjing 210093, China
E-mail: liangbin@nju.edu.cn; jccheng@nju.edu.cn
Prof. C.-W. Qiu
Department of Electrical and Computer Engineering
National University of Singapore
4 Engineering Drive 3, Singapore 117583, Singapore
E-mail: chengwei.qiu@nus.edu.sg
The ORCID identification number(s) for the author(s) of this article can be found under https://doi.org/10.1002/adma.201800257.

DOI: 10.1002/adma.201800257

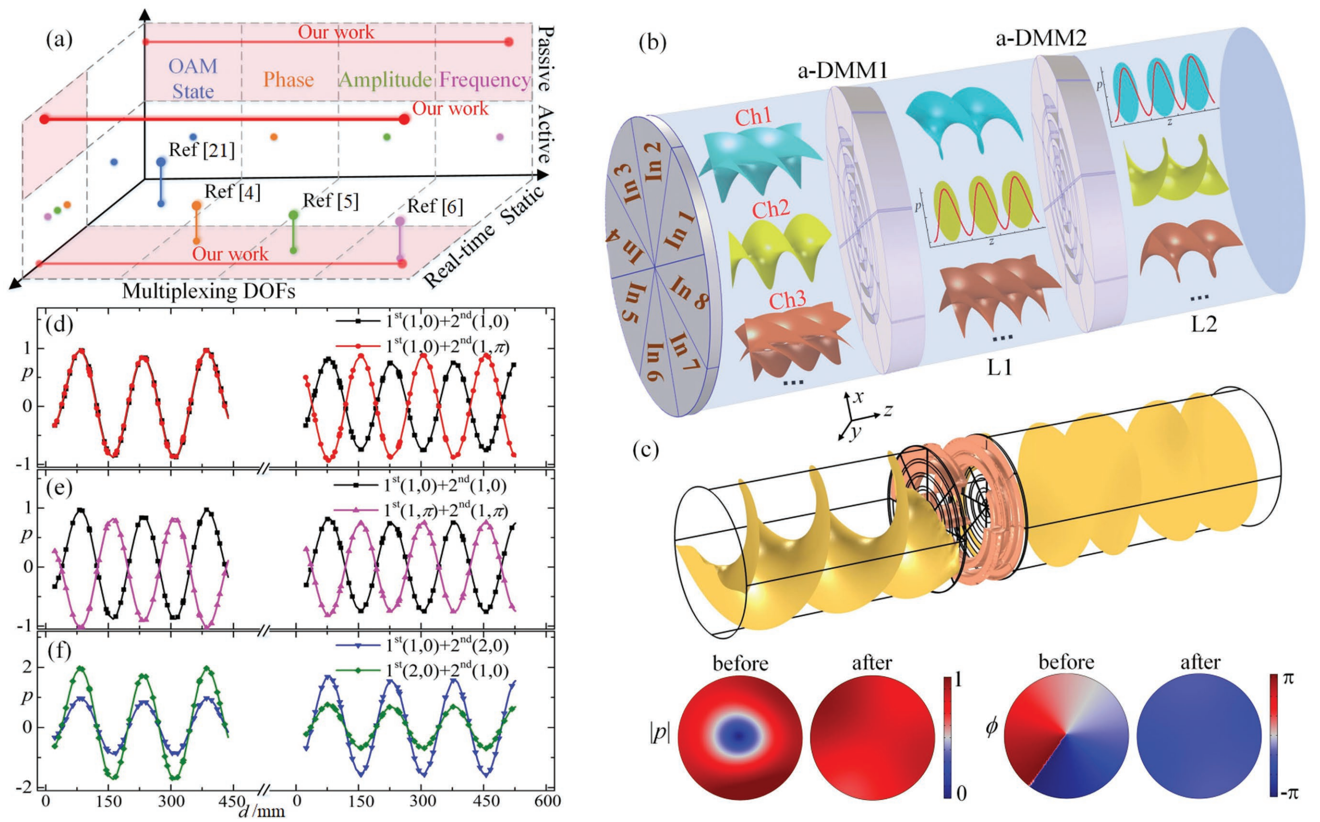

Figure 1. Concept of a-OAM beam can be considered as independent information carrier for multiplexing and demultiplexing. a) Comparisons among this work, the methods in ref. [21] and other milestone references. b) Schematic representation for multiplexing, the entrance is divided into eight sections, with each accessing to an individual input. For demultiplexing, twisted beams with null core are converted to updated a-OAM beams or plane wave (nonnull core). c) Equiphase surfaces of pressure p for the 1st order a-OAM beam transmitting through an a-DMM in waveguide. d–f) Normalized spatial distributions of p along centerline in regions L1 and L2 with different input signals. a-OAM, acoustic orbital angular momentum; In: input; Ch, channel; a-DMM, acoustic demultiplexing metasurface.

In this scheme (Figure 1b), twisted beams of different order m make up the multiplexing signal and propagate in an overlaid fashion as orthogonal channels. The multiplexing signal is expressed as $p(r,\theta,z,t)=\sum_m A_m(t)e^{i(m\theta+k_z z+\phi_m(t))}$, propagating along z direction (with the axial wavenumber k_z) in waveguide to avoid diffraction attenuation. The time-dependent amplitude $A_m(t)$ and phase $\phi_m(t)$ can be merged in the multilevel formats, suggesting the handy combination with preexisting multiplexing (e.g., WDM and TDM). We use the angular spectrum to yield the input p_{in} in emitting end (see Supporting Information), similar with that for calculating the profile in acoustic hologram.[28] The continuous p_{in} is discretized by dividing the entrance into eight sections, individually accessing to eight inputs controlled by different generators. As a result of the spatial multiplexing, the spectral efficiency can be enhanced by N, with N being the total number of twisted beams.

We propose a metasurface-based demultiplexing mechanism to separate beams with different m and thereby decode the data in each a-OAM channel. The mechanism is that, N layers of identical passive metasurfaces (denoted as a-DMMs) of a -1 OAM value are successively impressed, leading the order of all the transmitted a-OAM modes to be lowered by 1 (i.e., the OAM after the nth layer is $m-n$), and the output is detected by a single transducer at the center after each layer. Considering the doughnut-shaped intensity profile of a twisted beam, only by using m layers of a-DMMs can we remove the spiral phase of an mth order beam and observe a nonzero intensity at the core, while beams of other orders still remain the null core. Therefore, we can precisely detect the information encoded onto the mth order beam exclusively after the mth a-DMM by a single transducer. An example is illustrated in Figure 1c, which is the equiphase surface of the 1st a-OAM beam before and after an a-DMM in waveguide. Here, the metasurfaces of the -1 OAM value have a θ – dependent effective wavenumber k_{eff} by tuning its geometry, and the details of the parameters are provided in the Supporting Information.

We present a demonstration via merging the data in multilevel phase, i.e., differential binary phase shift keying (DBPSK), and amplitude, i.e., amplitude shift keying (ASP) formats. The notation mth ($A_m(t)$, $\phi_m(t)$) indicates the mth a-OAM beam with the amplitude $A_m(t)$ and phase $\phi_m(t)$ hereafter. The multiplexing signal is the superposition of the 1st and 2nd a-OAM beams carrying the objective data. Acoustic pressure p along central axis in regions L1 and L2 after demultiplexed by the a-DMMs are illustrated in Figure 1d–f as function of distance d from the output surfaces of corresponding layers, where the multiplexing signals carry different information. For better comparison, all the values are normalized by the maximum $|p|$ in the 1st (1, 0) + 2nd (1, 0) case. The objective data carried by the 1st and 2nd beams are perfectly restored after demultiplexed by the two a-DMMs in regions L1 and L2, respectively. For example, in Figure 1d the received signals in L2 have a phase shift of π which is exactly the phase difference in the 2nd a-OAM beams between the two input signals, and in Figure 1f the amplitude in the 1st(2, 0) + 2nd(1, 0) case is two times (half) of that in the 1st(1, 0) + 2nd (2,0) case in L1 (L2). The pressure transmittance is 91.5% after one a-DMM, which guarantees a high transmission. These results verify that the orthogonality between the a-OAM modes effectively avoids mode coupling and crosstalk in the spatially independent channels. Moreover, they substantially prove that the a-OAM is essentially orthogonal to the dimensions of phase and amplitude. Due to the resonant nature and consequent frequency selectivity of the metasurfaces,[16] only the a-OAM beams operating in the resonant frequency f_0 of the a-DMM can be converted to plane wave an d detected, which ensures the orthogonality with frequency as well. The frequency selectivity helps to simplify the terminal configuration when combined with the WDM where complicated equipment is required to filter,[29] increasing the speed and reducing the burden of the postprocessing.

We demonstrate the a-OAM multiplexing and demultiplexing via real-time communication. As a visualized example, we use the 1st and 2nd a-OAM beams as two channels Ch1 and Ch2, and independently encode each pixel of two pictures: images of letters "A" and "a," into the phase of a-OAM beams in DBPSK format as a binary data through numerical simulation. For real-time transfer, the multiplexing signal is in pulse modulation, with a central frequency f_0 = 2287Hz (period T_0), pulse period $20T_0$ and duty ratio 0.7, where each pulse cycle contains one-bit data. The eight inputs (Figure 1b) for generating the multiplexing signal and simultaneously enabling the two channels are displayed in **Figure 2**b. In receiving end, two a-DMMs and microphones (Mics) are cascaded to demultiplex and detect the signals in L1 and L2. The real-time signal in Ch1 (received in region L1) as function of time in each pulse period is partly plotted in Figure 2c, where the blue plane is the reference surface for phase comparing and data extracting in each cycle of the pulse-modulated signal. Data in other cycles and Ch2 are obtained in a similar way. The decoded data rows in Ch1 (1st beam) and Ch2 (2nd beam) are displayed in Figure 2a in comparison with the objective. With the detected dataflows where the binary information "0" and "1" represent two different colors of each pixel, two images are reconstructed as shown in Figure 2d,e, which undistortedly reproduce the pictures of letters "A" and "a."

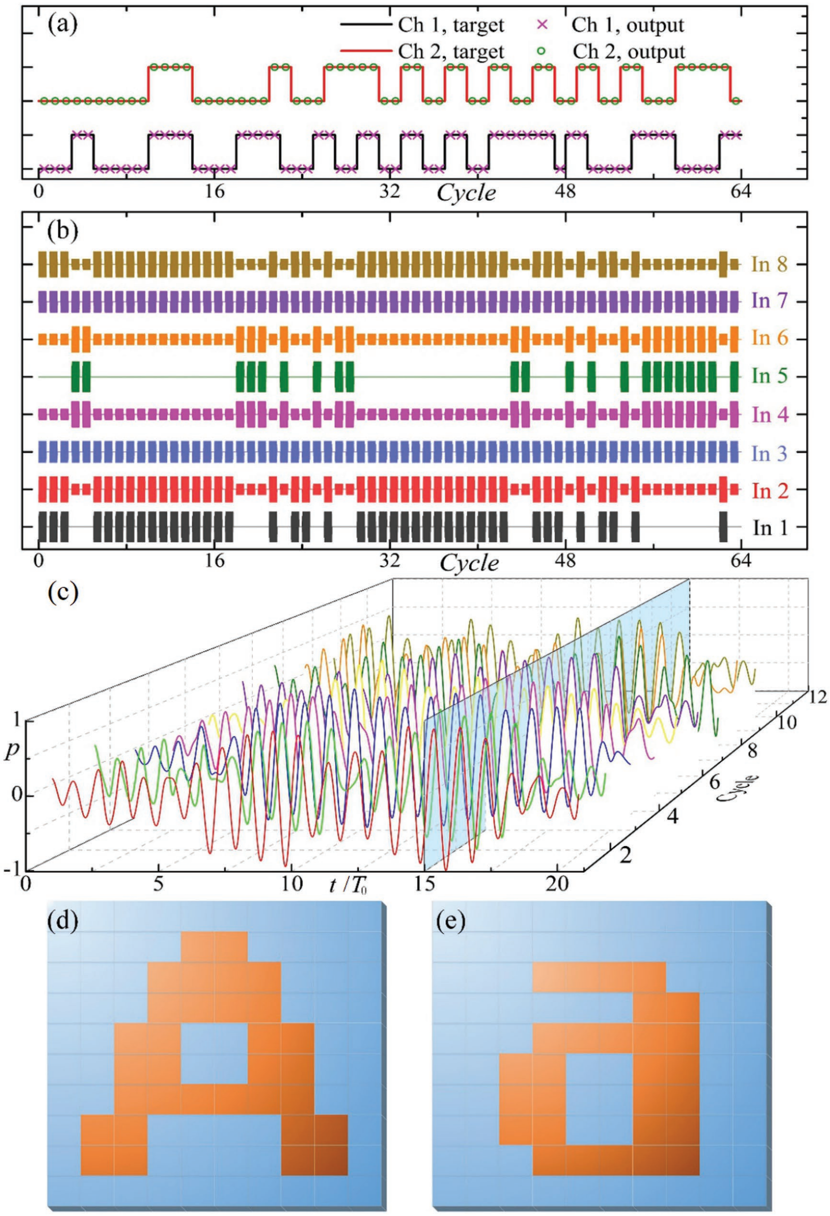

Figure 2. Real-time communication. Multiplexing signal contains 1st and 2nd a-OAM beams serving as Ch1 and Ch2. a) Comparison between the objective and received output. b) Inputs in the eight sections for generating the multiplexing signal, simultaneously enabling the two a-OAM channels. The signals are in pulse modulation, with the central frequency f_o (period T_o), pulse period $20T_o$, and duty ratio 0.7. Each pulse cycle contains one-bit of data. c) Part (first 12 cycles) of the received signal as function of time in each pulse period in L1. The blue plane is the reference surface for extracting information in each cycle of the pulse-modulated signal. d,e) Images independently retrieved from the received data carried by a-OAM beams in Ch1 and Ch2.

Experiments to verify the real-time OAM-based communication are conducted in cylindrical waveguide with two a-DMMs made of UV resin and two Mics centrally placed in L1 and L2 (**Figure 3**a,b). The length of the waveguide is 4 m and the distance between the two a-DMMs is 2.5 m, corresponding to 27 and 16 λ, respectively. As a proof-of-concept experiment,

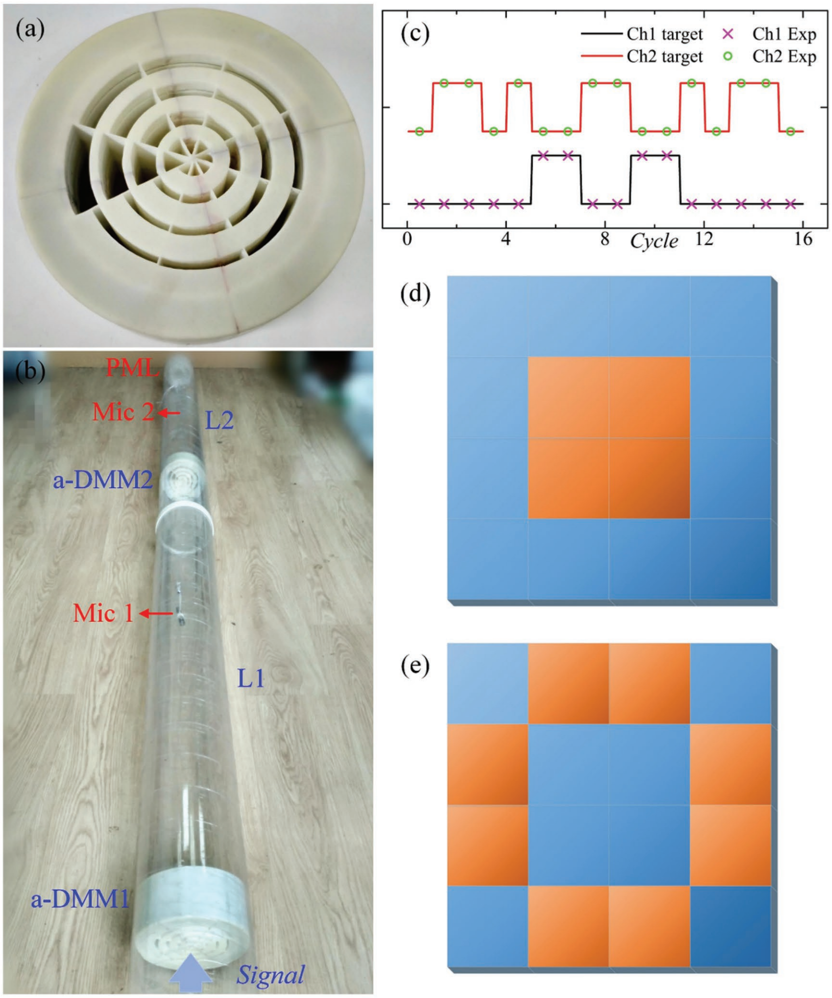

Figure 3. Experiments for the real-time a-OAM-based communication. a) An a-DMM sample. b) Experimental setup. The multiplexing signal is synthesized and propagates in waveguide. Two a-DMMs are sequentially placed and two Mics are centrally situated in L1 and L2. c) Experimentally received data flow in Ch1 and Ch2 comparing with the objective. d,e) Reconstructed images with the data received in Ch1 and Ch2. Mic, microphone; PML, perfect match layer.

we consider the independent transmission of two images each with 4 × 4 pixels encoded onto the 1st and 2nd a-OAM beams. The experimentally received data extracted from the real-time transmitted signals in Ch1 and Ch2 are displayed in Figure 3c, comparing with the objective. Perfect reconstruction of the images retrieved from the two dataflows is illustrated in Figure 3d,e, which demonstrates the experimental viability of the data transfer based on twisted beams.

Furthermore, we combine the a-OAM multiplexing with the multicarrier modulation (MCM) technology to increase the transmission efficiency within the limited available bandwidth, which is crucial to transfer the urgent information and particularly beneficial in the varying fading conditions.[30] The high-speed data stream is separated into several parallel flows of a relatively lower speed, encoded onto different a-OAM beams transmitting simultaneously, and then the decoded data are assembled accordingly. Here, we use the MCM to transfer an image of letters "NJU," by encoding the image pixels alternately into the 1st and 2nd beams. The assembled data stream measured experimentally, in comparison with the simulation results and the objectives are displayed in **Figure 4**a, where the inset partly shows the enlarged view of the comparison. Figure 4b shows the retrieved image with the received data both in simulation and experiment, which is the exact reproduction of the original picture. The combination of MCM and twisted acoustics would facilitate the high-speed data transfer and improve the efficiency of postprocessing.

To conclude, we propose and experimentally demonstrate a metasurface-based mechanism of twisted acoustics for the real-time, postprocess-free, sensor scanning-free, and high-capacity communication, where twisted beams of different OAM values serve as the spatially independent channels to carry information, with the compatibility with preexisting multiplexing. Subwavelength metasurfaces are employed as the passive and efficient demultiplexing component for direct and prompt data decoding with single transducer. It is noteworthy that the proposed scheme is universal since data transfer with this method is in principle not restricted by the number of OAM beams or transmitting distance, which can be extended to contain more a-OAM channels. More a-DMMs could be cascaded in the receiving end to efficiently demultiplexing more a-OAM beams. For a system of even more a-OAM channels, we can split the multiplexing signals into two parallel ends and employ a series of a-DMMs of -2 OAM values to separately demultiplexing the odd and even orders of a-OAM modes, which helps to ulteriorly increase the efficiency. Further improvements might lead to encode data by higher-order shift keying to achieve high capacity and spectral-efficiency acoustic communication.

In addition, the a-OAM-based communication would be resistant to eavesdropping. Conventionally, the signal would be covertly intercepted with additional receiver due to the atmospheric scattering, which requires extra mathematical encryption. Our scheme offers the security enhancement as it is difficult to read the data with an offset detector.[9] In other words, the recovery is nontrivial. Moreover, although the OAM-based acoustic communication is demonstrated for airborne sound, our scheme provides a paradigm for OAM multiplexing in water, which may in principle extended to underwater communication. However, the different environment requires alternative materials to fabricate the metasurfaces for providing a sufficient contrast of the impedance with that of water, or alternative media for resonance, such as the soft media. With the intrinsic orthogonality, high-decoding efficiency and accuracy,

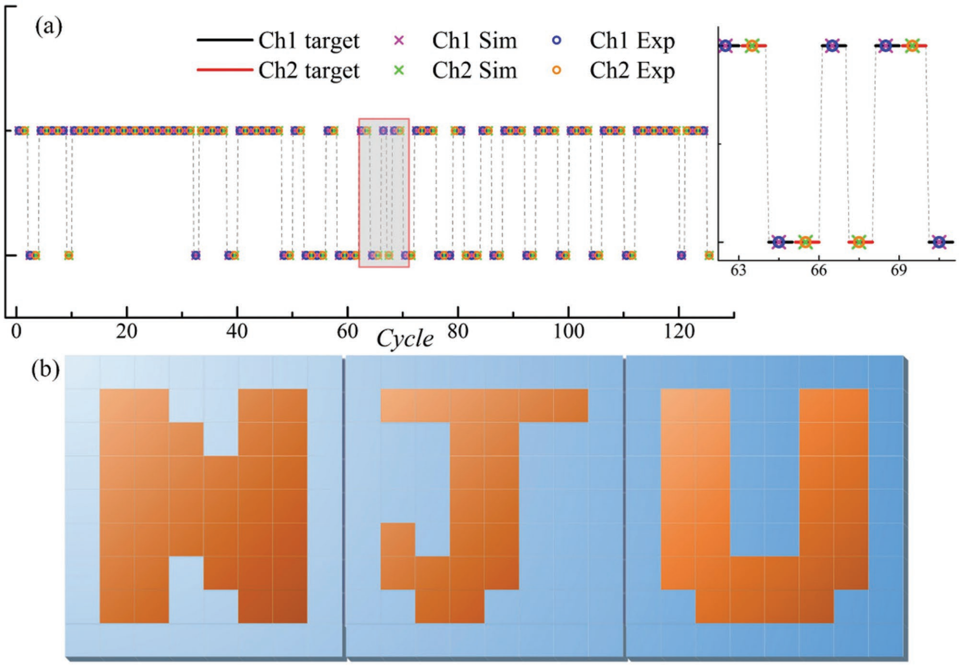

Figure 4. MCM with a-OAM beams. a) Experimentally and numerically received high-speed data flow, which are separately and parallel encoded in Ch1 and Ch2 and assembled after independently demultiplexed by the a-DMMs, in comparison with the objective. Inset, enlarged view of the data stream. b) Image reconstructed from the assembled data stream both in simulation and experiment.

increased integration density and the potential resistance to eavesdropping, twisted acoustics with OAM would take acoustic communication to new heights, providing potential to improve the capacity and security of information transmission.

Supporting Information

Supporting Information is available from the Wiley Online Library or from the author.

Acknowledgements

This work was supported by the National Key R&D Program of China, (Grant No. 2017YFA0303700), National Natural Science Foundation of China (Grants Nos. 11634006 and 81127901), and a project funded by the Priority Academic Program Development of Jiangsu Higher Education Institutions.

Conflict of Interest

The authors declare no conflict of interest.

Keywords

acoustic vortex metasurfaces, multiplexing and demultiplexing, orbital angular momentum, real-time information transfer

Received: January 11, 2018
Revised: February 10, 2018
Published online: March 30, 2018

[1] M. Stojanovic, *IEEE J. Oceanic Eng.* **1996**, *21*, 125.
[2] D. B. Kilfoyle, A. B. Baggeroer, *IEEE J. Oceanic Eng.* **2000**, *25*, 4.
[3] A. C. Singer, J. K. Nelson, S. S. Kozat, *IEEE Commun. Mag.* **2009**, *47*, 90.
[4] M. Stojanovic, J. A. Catipovic, J. G. Proakis, *IEEE J. Oceanic Eng.* **1994**, *19*, 100.
[5] H. Ochi, Y. Watanabe, T. Shimura, *Jpn. J. Appl.* **2004**, *43*, 3140.
[6] L. Freitag, M. Stojanovic, S. Singh, M. Johnson, *IEEE J. Oceanic Eng.* **2001**, *26*, 586.
[7] W. Li, J. C. Preisig, *IEEE J. Oceanic Eng.* **2007**, *32*, 927.
[8] G. Gibson, J. Courtial, M. J. Padgett, M. Vasnetsov, V. Pasko, S. M. Barnett, S. Franke-Arnold, *Opt. Express* **2004**, *12*, 5448.
[9] N. Bozinovic, Y. Yue, Y. Ren, M. Tur, P. Kristensen, H. Huang, *Science* **2013**, *340*, 1545.
[10] J. Wang, J. Y. Yang, I. M. Fazal, N. Ahmed, Y. Yan, H. Huang, Y. Ren, Y. Yue, S. Dolinar, M. Tur, A. E. Willner, *Nat. Photonics* **2012**, *6*, 488.
[11] T. Lei, M. Zhang, Y. Li, P. Jia, G. N. Liu, X. Xu, Z. Li, C. Min, J. Lin, C. Yu, H. Niu, X. Yuan, *Light: Sci. Appl.* **2015**, *4*, e257.
[12] N. Zhang, X. C. Yuan, R. E. Burge, *Opt. Lett.* **2010**, *35*, 3495.
[13] E. Nagali, F. Sciarrino, F. Martini, L. Marrucci, B. Piccirillo, E. Karimi, E. Santamato, *Phys. Rev. Lett.* **2009**, *103*, 013601.
[14] J. Leach, J. Courtial, K. Skeldon, S. M. Barnett, S. Franke-Arnold, M. J. Padgett, *Phys. Rev. Lett.* **2004**, *92*, 013601.
[15] B. T. Hefner, P. L. Marston, *J. Acoust. Soc. Am.* **1999**, *106*, 3313.
[16] X. Jiang, Y. Li, B. Liang, J. C. Cheng, L. K. Zhang, *Phys. Rev. Lett.* **2016**, *117*, 034301.
[17] L. K. Zhang, P. L. Marston, *Phys. Rev. E* **2011**, *84*, 065601.
[18] T. Wang, M. Ke, W. Li, Q. Yang, C. Qiu, Z. Liu, *Appl. Phys. Lett.* **2016**, *109*, 123506.
[19] Z. Y. Hong, J. Zhang, J. B. W. Drinkwater, *Phys. Rev. Lett.* **2015**, *114*, 214301.
[20] D. Baresch, J. L. Thomas, R. Marchiano, *Phys. Rev. Lett.* **2016**, *114*, 024301.

[21] C. Shi, M. Duboisa, Y. Wang, X. Zhang, *Proc. Natl Acad. Sci. USA* **2017**, *114*, 7250.
[22] B. Xie, K. Tang, H. Cheng, Z. Liu, S. Chen, J. Tian, *Adv. Mater.* **2017**, *29*, 163507.
[23] L. L. Huang, H. Mühlenbernd, X. W. Li, X. Song, B. F. Bai, Y. T. Wang, T. Zentgraf, *Adv. Mater.* **2015**, *27*, 6444.
[24] F. Monticone, C. A. Valagiannopoulos, A. Alù, *Phys. Rev. X* **2016**, *6*, 041018.
[25] N. I. Zheludev, Y. S. Kivshar, *Nat. Mater.* **2012**, *11*, 917.
[26] C. Shen, Y. Xie, N. Sui, W. Wang, S. A. Cummer, Y. Jing, *Phys. Rev. Lett.* **2015**, *115*, 254301.
[27] Y. Li, C. Shen, Y. Xie, J. Li, W. Wang, S. A. Cummer, Y. Jing, *Phys. Rev. Lett.* **2017**, *119*, 035501.
[28] K. Melde, A. G. Mark, Q. T, P. Fischer, *Nature* **2016**, *537*, 518.
[29] L. J. Cimini, *IEEE Trans. Commun.* **1985**, *33*, 665.
[30] M. S. Yee, M. Sandell, Y. Sun, *Proc. IEEE Veh. Technol. Soc.* **2004**, *3*, 1275.